Investigation of EDM Characteristics of Nickel-based Heat Resistant Alloy

Sin Ho Kang*, Dae Eun Kim
Department of Mechanical Engineering, Yonsei University, 134, Shinchon-dong, Seodaemoon-ku Seoul 120-749, Korea

The EDM processing characteristics of one of the nickel-based heat resistant alloys, Hastelloy-X, were investigated under the various EDM conditions and analyzed in terms of surface integrity. This alloy is commonly used as a material for the hot gas path component of gas turbines and it is difficult to machine by conventional machining methods. The primary EDM parameter which was varied in this study were the pulse-on time. Since the pulse-on time is one of the main factors that determines the intensity of the electrical discharge energy, it was expected that the machining ratio and the surface integrity of the specimens would be proportionally dependent on the pulse-on duration. However, experimental results showed that MRR (material removal rate) and EWR (electrode wear rate) behaved nonlinearly with respect to the pulse duration, whereas the morphological and metallurgical features showed rather a constant trend of change by the pulse duration. In addition the heat treating process affected the recast layer and HAZ to be recrystallized but softening occurred in recast layer only. A metallurgical evaluation of the microstructure for the altered material zone was also conducted.

Key Words : Electrical Discharge Machining, Hastelloy-X, Pulse-on Time, Recast Layer, Surface Integrity

1. Introduction

Hastelloy-X, one of the Ni-based heat resistant alloys, has been a common material used as combustor components of land based gas turbines or aircraft engines due to its high-temperature corrosion/erosion resistance combined with excellent fabricability and weldability (Bradley, 1988). The combustor components are inevitably exposed to high thermal stress and a very corrosive environment simultaneously. Therefore, the material of the components should be capable of maintaining adequate mechanical and chemical characteristics in such a severe environment. Recently, progress in the gas turbine technology has improved the efficiency in a higher firing temperature. Consequently, the combustor components are made with the materials that have superior creep strength and corrosion resistant property (El-Wakil, 1984).

In addition, by forming cooling passages in the parts strategically based on heat transfer analyses, the temperature of the parts during the operation can be remarkably reduced even though the firing temperature is much higher than the melting point of the material (El-Wakil, 1984 ; Lee et al, 1999). The shape of the cooling holes are circular and the dimension of the holes depend on the component size. In most cases, the aspect ratio of the cooling hole is high and the number of cooling holes per part is large. Therefore, it is quite difficult to drill the cooling holes precisely and rapidly by traditional manufacturing processes. At the present, CNC Electrical Discharge

* Corresponding Author,
E-mail : shkang@kps.co.kr
TEL : +82-32-580-8245; **FAX** : +82-32-580-8283
Craduate School of Yonsei University, Korea Plant Service and Engineering Co. Ltd. 247, Gyeongseo-dong, Seo-gu, Incheon, Korea. (Manuscript **Received** March 19, 2003; **Revised** July 5, 2003)

Table 1 Nominal composition of Hastelloy-X (Wt%-sheet) (Stoloff, 1990)

Ni	Cr	Co	Mo	W	Fe	Mn	Si	C	Density	Melting Range
47	22.0	1.5	9.0	0.6	18.5	0.50	0.5	0.10	8.21 g/cm^3	1260-1355℃

Table 2 Mechanical properties of Hastelloy-X (Stoloff, 1990)

Property	21℃	93℃	204℃	316℃	427℃	538℃	649℃	760℃	871℃	982℃
Specific Heat (J/Kg·K)	485	—	—	500	—	—	585	—	700	—
Thermal Conductivity (W/m·K)	9.1	11.0	12.7	14.4	17.2	19.6	21.8	24.0	26.0	28.1
Mean Coefficient of Thermal Expansion ($\times 10^{-6}$/℃)	—	13.9	14.1	14.2	14.7	15.1	15.4	15.9	16.2	16.6
Dynamic Modulus of Elasticity (GN/m^2)	197	194	186	178	170	161	154	146	137	128
Yield Strength (0.2% offset) (MN/m^2)	360	—	—	—	—	290	275	260	180	110
Ultimate Tensile Strength (MN/m^2)	785	—	—	—	—	650	570	435	255	150

Table 3 100hr 0.2% creep strength of Hastelloy-X, MN/m^2 (Source : International Nickel Co.)

649C	704C	760C	816C	871C	927C	962C
140	90	55	35	22	13	8

Machining (EDM) is being widely applied in drilling the cooling holes. The workpiece material can affect the characteristics of the defects on the EDM processed surface. This is due to the fact that the transformation of the thermal energy from the electrode to the workpiece, dictated by machining parameters, is dependent on the physical properties of the workpiece material such as thermal conductivity and chemical composition (IAMS, 1980).

In this work, the machining characteristics of Hastelloy-X and the surface defects that appear under various EDM conditions were investigated. Tables 1 through 3 show the chemical composition and the mechanical properties of Hastelloy-X. The motivation of this study was to better understand how the surface integrity of the Ni-based Superalloy is affected by the EDM process. Thus, experimental investigations were carried out to analyze the altered material zone (hereafter referred to as AMZ) following the EDM process. The following sections describe the experimental work in detail.

2. Experimental Conditions

Hastelloy-X specimens were EDM processed under various conditions to investigate the effect of machining condition on the surface integrity of the workpiece. Four machining conditions were selected where the pulse-on time was varied while maintaining other parameters such as off time, peak current, and gap voltage constant. A 2.35 mm thick Hast-X sheet material was cut to a 32×100 mm rectangle and used as the workpiece specimens. The specimens were machined with a 16 mm diameter copper electrode for 150 seconds under the four machining conditions. Table 4 shows the selected machining conditions used in this study.

Since the machine was a plunge type EDM, flushing nozzles were installed and the kerosene

Table 4 Experimental machining parameters

Experimental EDM Conditions	Pulse On-Time	Pulse Off-Time	Machining Current (A)	Machining Time (S)	Duty Factor
Cond. #1	50	20	4~6	150	0.714
Cond. #2	100				0.833
Cond. #3	400				0.909
Cond. #4	600				0.952

dielectric fluid was sprayed to the machining area to attain better flushing of the debris. The electrode was connected to the positive polarity (+) and each machining process was continued for 150 seconds without any jumping movement of the ram. Some of the machined specimens were solution heat-treated to observe the differences of the AMZ between before and after the heat treatment.

After specimens were EDM processed, the following experimental techniques were employed for assessing the surface integrity of the Hast-X sheet material.

(1) Scanning Electron Microscopy (SEM): crater size, distribution, and the existence of microcracks were analyzed by observation of the surface and cross sectional layer of the specimen.

(2) Optical microscopy: sectional microstructures were compared before and after etching. In order to identify the phases and grain boundaries, specimens were etched by immersing in a 10% oxalic acid solution.

(3) Energy Dispersive Spectrometer (EDS): insertion of foreign objects in recast layers and splatters were observed as well as the chemical composition of the machined layers. In addition, this technique was also used for quantitative analysis of the change in the alloy among the layers.

(4) Surface roughness measurement: surface roughness in Ra (average roughness) was measured as a means to assess the surface profile change due to different machining conditions.

(5) Microhardness measurements (Knoop Hardness: HK): the hardness distribution was measured from the recast layer through the base metal of the sectional microstructure before and after heat treatment.

3. Experimental Results and Discussion

3.1 Size and density of the EDM marks

The specimens were EDM processed according to the specified conditions and their surface conditions were evaluated using microscopy. As shown in Figs. 1 and 2, as the pulse-on time increased, the crater diameter as well as the thickness of the recast layer increased. This can be based on the well-known fact that heat input to the workpiece surface increases as the pulse-on time increases although the machining current

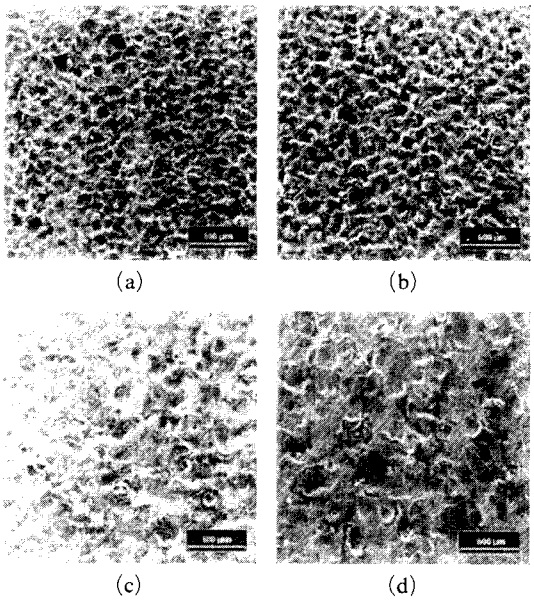

Fig. 1 SEM micrographs of EDM processed surface under 4 machining conditions: (a) EDM condition #1, (b) EDM condition #2, (c) EDM condition #3, (d) EDM condition #4

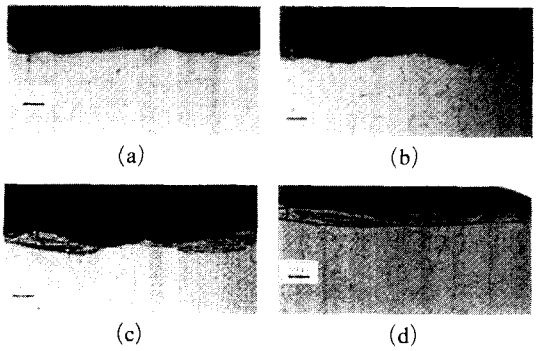

Fig. 2 Cross-sectional optical micrographs on EDM processed surface under 4 machining conditions : (a) EDM condition #1, (b) EDM condition #2, (c) EDM condition #3, (d) EDM condition #4

was maintained to be constant in this study (Fuller, 1989).

SEM observation of the specimens before heat treatment showed evidence of globular splatters and carbon deposits on the machined surfaces. Except some of the globular splatters that contained Cu element, since the electrode was copper, the chemical composition of the deposits and the EDM processed surface were found to be same as the base metal. An EDS analysis was conducted to identify the change in the alloy. The result indicate that there is a difference in the chemical composition between the copper electrode splatter and the base metal deposits, as shown in Fig. 3.

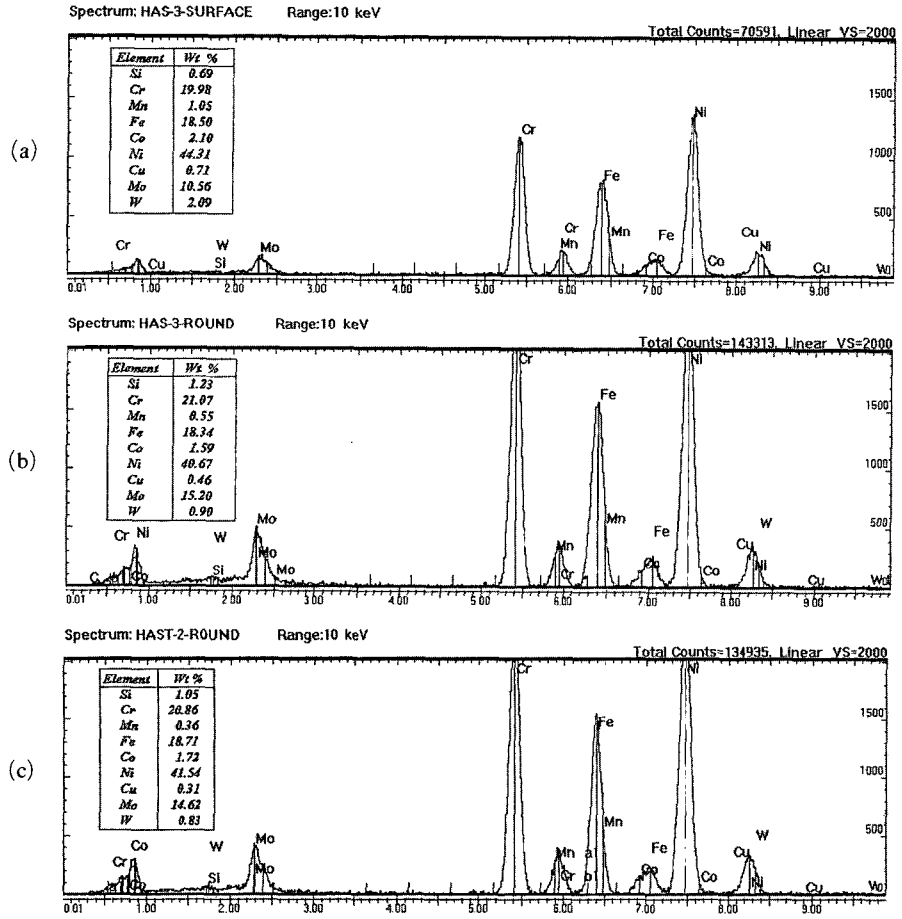

Fig. 3 EDS analysis to verify the change of alloy composition for : (a) EDS analysis results of recast on EDM processed surface of specimen #3, (b) EDS analysis results of deposit on the EDM processed surface of specimen #3, (c) EDS analysis results of deposit on EDM processed surface of specimen #2

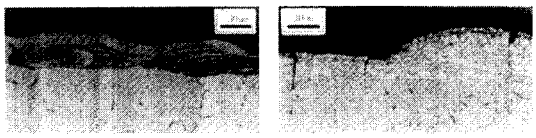

(a) (b)

Fig. 4 Comparison of micro structural change by solution annealing heat treatment for:
(a) Condition #1 (before heat treatment),
(b) Condition #3 (after heat treatment)

After the specimens were heat-treated, the rapidly resolidified amorphous layer converted into grains and boundaries just like a base metal. Although the grain size was smaller and closer than the substrate, the boundaries in the substrate linked up with the boundaries in the recast layer selectively. HAZ, which is one of the important components of AMZ created by EDM, was observed as a structurally different layer from the substrate whereas it was not clearly distinguishable before the specimens were solution heat treated. As reported by previous observation (IAMS, 1980), the thickness of the HAZ layer was approximately the same as that of the maximum thickness of the recast layer. After heat treatment, the M_6C type carbide densely appeared in the HAZ layer. Therefore, the three layers became more apparent after the solution heat treatment even though the morphology of the machined surface represented no changes. Figure 4 shows the optical micrographs of the cross-sectional views of the specimens before and after the heat treatment.

3.2 MRR, EWR and REW

The material removal rate (MRR) and electrode wear rate (EWR) in EDM are closely related to machining accuracy and productivity since the major mechanism of material removal is the erosion which occurs between the two poles. This is the reason why EDM is not a fast material removal process as the conventional machining methods. Moreover the accuracy of the EDM processed products will not be obtained if the relationship between MRR and EWR is not taken into consideration in determining the parameters of the EDM process.

In order to characterize the four experimental machining conditions, the weight change of the specimen and the electrode were measured after each machining step conducted utilizing a precision balance with a resolution of 10^{-5} gram. The relative electrode wear (REW) is defined as follows:

$$REW=\frac{EWR}{MRR}\times 100\%=\frac{\Delta We}{\Delta W_p}\times 100\%$$

where,

ΔW_e: Electrode wear weight per a minute (g/min)
ΔW_p: Workpiece wear weight per a minute (g/min)

The experimental results showed that machining condition #2 represented the highest MRR but with a relatively low EWR. Conditions #3 and #4 resulted in a negative REW, which means that some deposits generated during machining caused the weight of the electrode to increase. Figure 5 through 7 show the MRR, EWR and REW obtained from the four machining conditions, respectively.

To investigate the deposits on the electrode, SEM and EDS analyses were employed. It was found that the thickness of the deposited layer and EDM marks were dependent upon the pulse-on duration. Shorter pulse-on duration formed a thin layer and fine EDM marks while longer pulse-on duration formed a thick layer and coarse marks including more globular splatters. The deposits on the copper electrode, as reported in a previous study (Chen, et al. 1999), can be the result of solid solubilization and carbon diffusion when the machining is conducted in a carbonaceous dielectric fluid such as kerosene. Chen et al found that the carbide precipitated on the machined surface of Titanium alloy (Ti-6Al-4V) and the carbon deposited on the copper electrode. However in this study, the deposits on the electrode revealed by EDS analysis turned out to be a compound of the Hast-X workpiece and the copper electrode.

With regard to the negative REW obtained

under the machining conditions #3 and #4, it is believed that the amount of melted metal, which is subjected to instant vaporization, will be increased as the intensity of the discharge energy is increased. However in this experiment the intensity was governed by the pulse-on time only. This means that the heat input to both the electrode and workpiece increase when longer pulse on time is adopted. Accordingly, diffusive atmosphere on both surfaces become stronger whereas the off-time for sufficient vaporization in the gap is relatively short. Therefore, as observed in condition #4, a considerably larger portion of the fused metal was deposited and resolidified on the workpiece surface. This seems to be the reason why the lowest MRR was attained in condition #4.

On the opposite side, pyrographite which is dissolved from petroleum type dielectric fluid flow and adhere on the anodic electrode surface. Some part of the dissolved metal from the workpiece deposit on the copper electrode also. It is speculated that carbon and alloy from the workpiece form certain phases on the copper electrode which function as a wear resistant layer for the copper electrode. The increase in the electrode weight can be explained with this deposition effect. Figure 8 shows the deposits on the copper electrode and Figure 9 are the results of the EDS analysis of the deposits on the copper electrode surface.

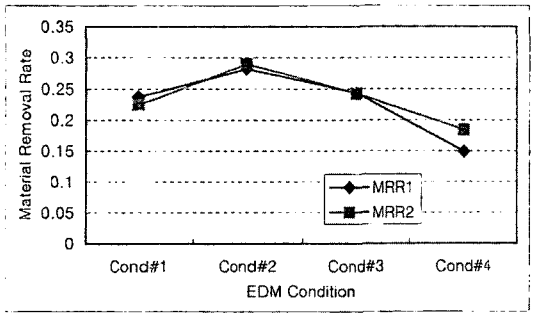

Fig. 5 Material removal rate with respect to EDM condition

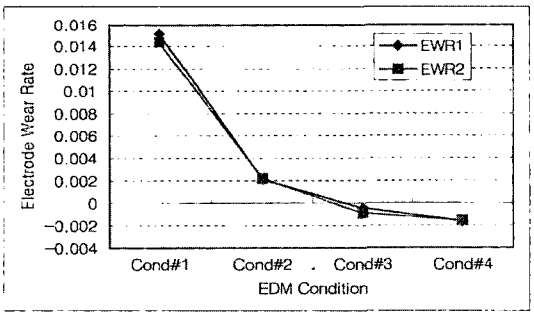

Fig. 6 Electrode wear rate with respect to EDM condition

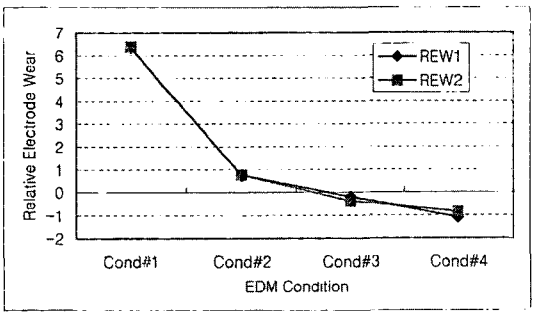

Fig. 7 Relative electrode wear with respect to EDM condition

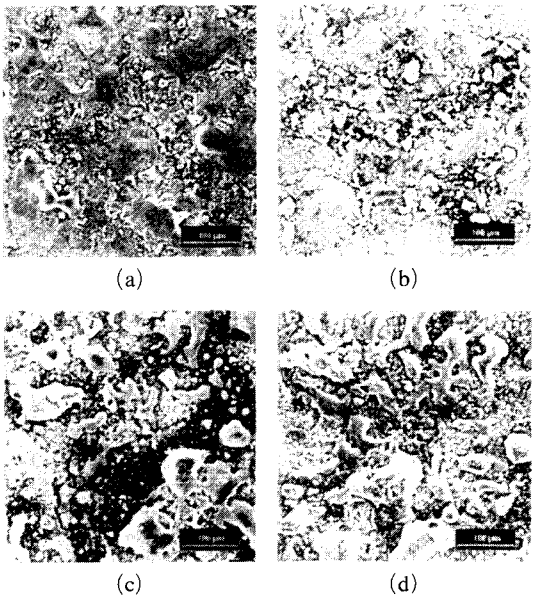

Fig. 8 SEM micrographs of eroded surface of the copper electrodes machined at various conditions: (a) EDM condition #1, (b) EDM condition #2, (c) EDM condition #3, (d) EDM condition #4

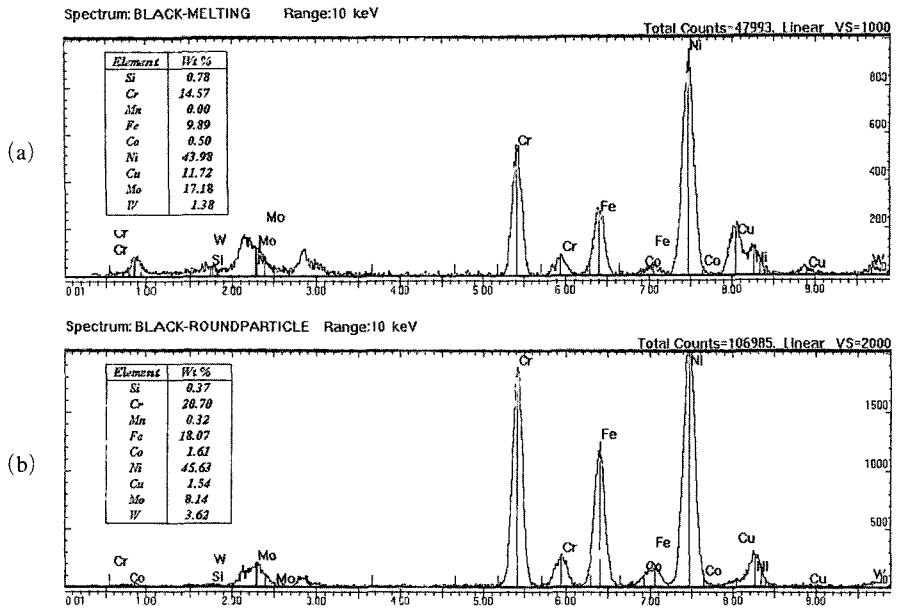

Fig. 9 EDS analysis results of the copper electrode : (a) Copper electrode surface after 150 second machining upon condition #4 and (b) Globular deposit on copper electrode surface after 150 second machining upon condition #4

3.3 Incidence of microcracks

It has been reported that the microcracks are caused by the high tensile residual stress present in the recast layer (Thomson, 1989 ; Rebelo et al., 1998). The recast layer seems to be formed as the fused metal rises around the circumference of the molten pool due to the expansive pressure while most of the molten metal is vaporized. At the final stage of the discharge transfer the molten metal spreads freely and covers the adjacent area by this expansion pressure. When the pulsated plasma ends and the gap between the two electrodes recover its dielectric property as soon as the fluid floods back, the spread molten metal is chilled immediately. Therefore, the spread metal which is initially in a stress-free state is subject under a tensile stress due to rapid contraction and remain as a resolidified layer on the surface. There has been a study which suggests that cracking occurs at the area with the largest tensile stress and the stress can be released by the formation of adjacent cracks (Thomson, 1989 ; Gadalla et al., 1991).

In this study, the largest amount of microcracks occurred in Hast-X when the specimens were processed under EDM condition #4, which left the thickest recast layer and widely distributed cracks. On the other hand EDM condition #1 resulted in the least number of cracks. Table 5 shows the number of cracks under each machining condition. Once the microcracks were formed, they neither disappeared nor diminished even after the heat treatment process (refer to Figure 10).

Table 5 Comparison of crack numbers with respect to EDM conditions

Condition No.	Before Heat Treatment	After Heat Treatment
1	3EA	11EA
2	13EA	17EA
3	65EA	55EA
4	70EA	60EA

For the solution heat treatment, specimens were put into a vacuum furnace and heated up to 1175℃ and maintained for 30 minutes. Then, the specimens were rapidly cooled to ambient temperature according to the material specification. It was found that gap of the microcracks

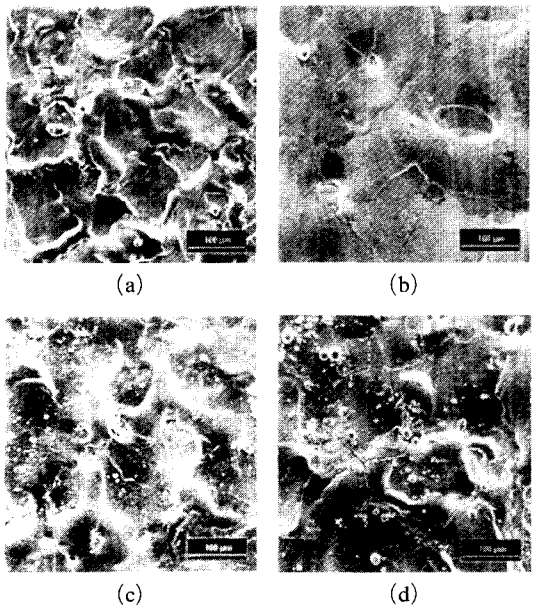

Fig. 10 Comparison of SEM micrographs of machined surfaces at mildest and the severest conditions:
(a) Condition #1 (before heat treatment),
(b) Condition #4 (before heat treatment),
(c) Condition #1 (after heat treatment),
(d) Condition #4 (after heat treatment)

became up to 2.5 times wider after the heat treatment. This evidently suggests that the tensile stress existing around the cracks as well as the extremely high hardness of the surface is released by the heat-treating process.

3.4 Surface roughness measurement

As a means to access the surface integrity of the EDM processed specimens, the surface roughness values were measured. A precise surface roughness measurement can be performed on the EDM processed surfaces by averaging of values taken by a stylus type measuring device in different directions (IAMS, 1983). Using a commercial surface profilometer (Surftest 301-Mitutoyo), the surface roughness of machined surfaces before and after the heat-treatment process were measured. The deviations in the measurement values within the 20 mm diameter area of each machined specimen were quite large. However, the trend of the surface roughness varied with respect to the

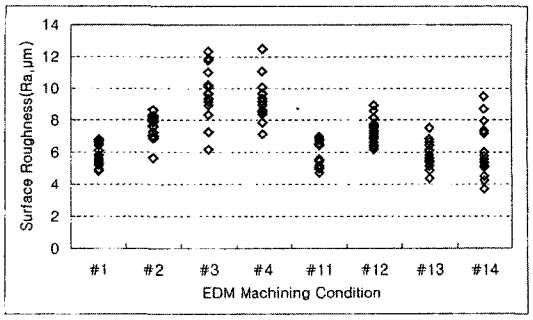

Fig. 11 Roughness distribution on EDM processed surfaces (#1~#4: before heat treat, #11~#14: after heat treat)

EDM condition. It was clearly evident that better surface finish was obtained when shorter pulse-on time was adopted. This observation can be well explained by the empirical equation: $Ra = k[I * t]^{\alpha}$ where the constants k and α depend on the tool and workpiece material combination (Rebelo et al, 1998). Figure 11 shows the roughness distributions measured on the machined area of each specimen.

3.5 Microhardness measurement

Hardness is an important property which is readily altered by the EDM process. In this work the hardness values were measured for the machined specimens. The hardness numbers on the Knoop scale with 25 kgf preloading before the heat treatment process were high enough to reach up to 881 on average in the recast layer. The hardness of HAZ was measured to be 286, which was higher than the hardness of the base metal which was 245. The hardness of the recast layer remarkably decreased after the solution annealing heat treatment process and eventually fell below the hardness of the base metal. This phenomenon seems to be caused by the residual stress in the recast layer which was mostly released by the heat treatment process. Unlike the state before the heat treatment where there were no visible grains, it was verified that very fine grains appeared during recrystallization.

As noted in a previous study, in tool steel the hardness of the recast layer usually increased by martensite precipitation due to the extra carbon

from the carbonaceous dielectric fluid and/or graphite electrodes (Fuller, 1989; Thomson, 1989). In the solid-solution strengthening of Ni based alloy, unlike tool steels, it is believed that the amorphous phase is predominant in the resolidified layer after very rapid quenching is experienced during the pulse off period. Furthermore, within such a short time the resolidified material can form neither grains nor precipitations such as carbides.

This amorphous phase feature seems to be reasons why the top layer of EDM processed surface has an extremely high hardness and a non-etchable characteristic as well. With respect to HAZ, the hardness of HAZ exhibited slightly higher values than that of the base metal before the heat treatment process. This result does not coincide with the findings of previous studies on tool steels, because of the different hardening mechanisms between solid-solution strengthening superalloy and tool steel. The Hast-X is normally used as a solution annealed alloy with its exceptional resistance to oxidation and age hardenability. Thus, Hast-X can precipitate the secondary phase after prolonged exposure at elevated service temperature. Also, the overheated zone just beneath the recast layer precipitates the secondary phase such as γ' and carbides so that the zone exhibits the same effects as age hardening.

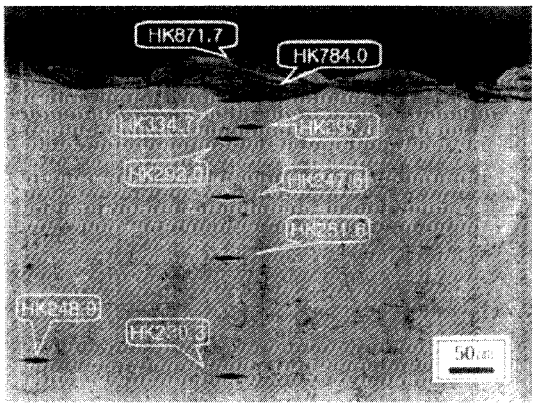

Fig. 12 Micro hardness indentation profile in the cross-sectioned specimen (EDM condition #3, before heat treatment)

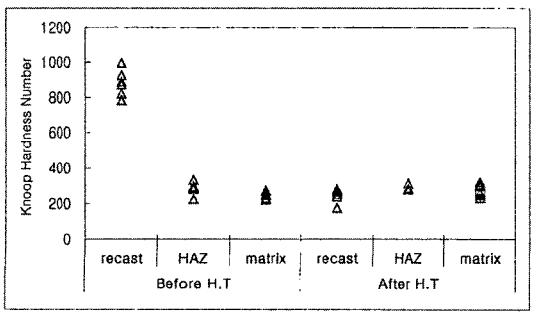

Fig. 13 Hardness distribution on EDM processed surface

Through SEM and EDS analyses it was found that more carbide particles existed in the HAZ than in the substrate. Although the hardness in the recast layer dropped sharply after the solution heat treatment process, there were no significant changes found on the hardness depth profile curve through HAZ and the substrate. Figures 12 and 13 show the hardness distribution on the cross-sectional area of the machined specimen.

4. Conclusions

Experimental investigation of the EDM process performed on Hast-X sheet material under four machining conditions revealed various machining characteristics that were dependent on pulse-on duration and the thermal properties of the workpiece. Conclusions obtained from this work may be summarized as follows:

(1) Machining condition #2 represented the highest MRR and relatively low REW, while #3 and #4 showed low MRR with negative REW. Carbide deposit was found on the copper electrode surface which formed like a coated layer that varied with pulse-on duration in terms of the amount of deposits.

(2) The combination of the longer pulse-on time and short pulse-off time, which is correspons to condition #4, resulted in relatively poorer surface integrity than the condition with a shortest pulse-on time. With respect to machining accuracy and productivity, condition #2 was found to be the most suitable for machining Hast-X material among the 4 conditions used in this study.

(3) For all machining conditions, microcracks were formed. The pulse-on time also affected the

number of microcracks and the thickness of AMZ ; for longer pulse-on time, more micro cracks formed and the AMZ was thicker. In all cases, microcracks existed in recast layers and they did not disappear or diminish by the solution annealing heat treatment process.

(4) Before the heat treatment, the recast layer showed a very high microhardness, whereas HAZ and base material showed similar values. The hardness value of the recast layer was similar to that of the base material after the solution annealing heat treatment. However, the hardness of HAZ remained practically unchanged, the value being 286 HK and 290 HK before and after the heat treatment, respectively.

References

Bradley, E. F., 1988, *Superalloy-A Technical Guide*, ASM International, pp. 14~29.

Chen, S. L., Yan, B. H. and Fuang, F. Y., 1999, "Influence of Kerosene and distilled Water as Dielectrics on the Electric Discharge Machining Characteristics of Ti-6Al-4V," *J of material processing Technology*, 87, pp. 107~111.

El-Wakil, M. M., 1984, *Powerplant Technology*, McGraw-Hill International Editions.

Fuller, J. E., 1989, "Electrical Discharge Machining," *Metals Handbook*, 9th Ed., Vol. 16, ASM International, pp. 557~564.

Gadalla, A. M., Bozukurt, B. and Faulk, N. M., 1991, "Modeling of thermal Spalling During Electrical Discharge Machining of Titanium Diboride," *Journal of the American Ceramic Society*, Vol. 74, No. 4, pp. 801~806.

Institute of Advanced Manufacturing Science (IAMS), Inc., 1980, "Surface Integrity," *Machining Data Handbook*, 3rd Ed., Vol. 2, pp. 18-98~18-106.

International Nickel Co., Nickel Base Alloys, Quoted in Wlodek, S. T. and Boone, D. H., 1997, *Superalloy Course Volume 1*, BWD Turbines LTD.

Lee, D. H. and Cho, H. H., 2000, "Heat Transfer Characteristics on Effusion Plate in Impingement/Effusion Cooling for Combustor," *Proceedings of KSME*, Vol. 24, 3, pp. 435~442.

Rebelo, J. C., Dias, A. M., Kremer, D. and Lebrun, J. L., 1998, "Influence of EDM Pulse Energy on the Surface Integrity of Martensitic Steels," *Journal of Material processing Technology*, 84, pp. 90~96.

Stoloff, N. S., 1990, "Wrought and P/M Superalloys," *Metals Handbook*, 10th Ed., Vol. 1, ASM International, pp. 950~980.

Thomson, P. F., 1989, "Surface Damage in Electrodischarge Machining," *Material Science and Technology*, Vol. 5, pp. 1153~1157.